SUPPLEMENTARY MATERIAL
Evaluating the response of hydrological stress indices using the CHyM model over a wide area in central Italy

S.1 Detailed geological description of the study area

The Tiber River, the widest in central Italy, is characterized by a total drained surface area of approximately 17,500 km^2, distributed along 2°3' of latitude. The Tiber originates in Monte Fumaiolo, in Tuscany (1,268 m a.s.l.), and flows for more than 400 km, before emptying into the Tyrrhenian Sea at Ostia. More than 90% of the basin surface is within the regions of Umbria and Lazio, while small parts of other regions, including Abruzzo, Molise, and Tuscany, are also encompassed in the catchment area. The morphology of the Tiber basin has undergone significant change over geological time. Its present natural structure is due to the effects of volcanic deposition during the Quaternary period [46]. While most rivers in central Italy have a transverse course, the main path of the Tiber is longitudinal. The basin is delimited by the Apennines to the east, where the main peaks of the study area are located (the highest peak is Mount Velino, in the Abruzzo region, at 2,487 m a.s.l.). To the south, the basin is bounded by the volcanic system of the Alban Hills, while to the west it is characterized by lower mountain ridges, with altitudes ranging from Mount Amiata at 1,734 m a.s.l. to the Tolfa Mountains at 616 m a.s.l. The north-western part is delimited by the Arno basin (Mount Cetona, 1,148 m a.s.l.) and the hill systems around Lake Trasimeno, the latter of which is included in the catchment area. After an initial torrential regime, the Tiber crosses a series of plains and valleys located at different topographical altitudes, until it reaches its final section, from Rome to the mouth, characterized by a flat course. Along its course, the Tiber receives hydric contributions from its tributaries, which contribute to its discharge. From a geographical and morphological perspective, the basin is generally divided in four sub-basins [50], including, from north to south i) the upper-Tiber basin (drainage area 6,077 km^2), which encompasses the upstream area from the Corbara reservoir (42.703˚N 12.231˚E), built in 1962. This area is characterized by poorly permeable clayish or sandstone deposits, alternated with fluvio-lacustrine sediment from ancient lakes; ii) the Paglia/lower-Tiber sub-basin (drainage area 5,343 km^2), which is characterized by terrain of varying permeability. In the north-western part of the Tiber watershed, the Paglia catchment, in particular, is mainly impermeable due to the presence of clay, while the lower-Tiber course is highly permeable due to the presence of limestone; iii) the Nera basin (drainage area 4,280 km^2), which is predominantly characterized by calcareous terrain with high permeability; and iv) the Aniene basin (drainage area 1,446 km^2), which is a karstic environment with high infiltration rates. While the tributaries to the east are mainly karstic and experience regular discharge throughout the year, the western drainage regime is seasonal with the discharge maxima occurring during the rainy seasons of fall and winter. Mean discharge of the Tiber, measured in Rome, ranges from 225 to 324 m^3/s.

The Tiber basin is heavily exploited for hydroelectric power, with 23 large reservoirs and 36 minor hydropower plants located in the area [48]. Of these, 11 dams are higher than 15 m or have a reservoir volume greater than 10^6 m^3 and are, therefore, classified as "large dams" (Italian Law no. 584/1994). The Corbara Dam is considered the most important reservoir. It significantly affects streamflow regulation in the middle and lower courses of the river and plays an important role in flood routing. For example, Bencivenga et al. [51] estimated a reduction of almost 400 m^3/s of peak discharge in Rome during a severe flood that occurred on 3 February 1989, due to upstream regulation by the Corbara Dam. During the same event, flood propagation was delayed by 18 hours. The discharge regime of the Tiber is classified by Frosini [52] as "Apennine sublittoral".

To the north of the Tiber river mouth are the coastal basins of the Arrone and Marta catchments, and the coastal area north of the Arrone outlet, which is characterized by short moats. The Arrone River originates from Bracciano Lake, which makes a negligible contribution to total runoff. Although the catchment extension is very small (~138 m^2), the basin morphology is complex, due to the numerous volcanic layers that intercept its main course.

The Liri-Garigliano basin flows through Lazio, Abruzzo, and Campania before flowing into the Tyrrhenian Sea. The northern area includes Fucino Lake, an ancient 150 km^2 wide swampland, reclaimed at the end of the 19th Century and today exploited for intensive agriculture. It is delimited to the south by the Mainarde massif, which divides the Liri-Garigliano from the Volturno watershed. The northern watershed is also delimited by the Albani Hills and the Apennines chain of Abruzzo. The Liri River originates in the northern part of the catchment, in the Simbruini Mountains (995 a.s.l.). After 60 km, the Liri joins the Garigliano. The total length of the Liri-Garigliano is 164 km. The Sacco River is a tributary of the Liri and the Cosa River is, in turn, a tributary of the Sacco; both flow across the northern area of the basin.

The Liri-Garigliano basin has a variety of characteristics, depending on acclivity. The lower course is mainly flat and composed of alluvial deposits. The hill area, which accounts for 38% of the basin area, includes the north-west sector. This is characterized by irregular slopes, with an average gradient of 10–35%. It is mainly composed of volcanic and flysch deposits, and clay predominates. From an anthropic perspective, it is the most important portion of the territory as it is the most densely populated area and rich in croplands. Finally, the mountainous area has an average gradient of 25–35% and encloses all the slopes bordering the basin in the north, north-east and east sectors, including the highest parts of the Liri Valley. This area accounts for approximately 44% of the entire territory.

SUPPLEMENTARY MATERIAL
Evaluating the response of hydrological stress indices using the CHyM model over a wide area in central Italy

TIBER BASIN		
UPPER COURSE		
STATION NAME	***COORDINATES***	***CRITICALITY THRESHOLDS***
Pistrino	43.497; 12.161	n.d.
Lupo	43.482; 12.184	n.d.
Serrapartucci	43.334; 12.413	n.d.
Mocaiana	43.371; 12.459	n.d.
Macerone	43.197; 12.069	n.d.
Paganico	43.128; 12.031	n.d.
Pianello	43.144; 12.566	OT: 2.00 m
		MT: 2.60 m
		HT: 2.80 m
Bastia Umbra	43.061; 12.542	n.d.
Bettona Q.A.	43.017; 12.541	OT: 3.60 m
		MT: 4.30 m
		HT: 4.50 m
Valtopina	43.047; 12.756	OT: 1.80 m
		MT: 2.00 m
		HT: 2.30 m
Nocera Scalo	43.099; 12.767	n.d.
Ponte Rosciano	43.022; 12.439	OT: 4.20 m
		MT: 4.90 m
		HT: 5.10 m
Monticelli	43.013; 12.262	n.d.
Ponticelli	42.930; 11.969	OT: 2.00 m

SUPPLEMENTARY MATERIAL

Evaluating the response of hydrological stress indices using the CHyM model over a wide area in central Italy

		MT: 2.60 m
		HT: 3.00 m
Ponte Santa Maria	42.896; 12.021	OT: 3.20 m
		MT: 4.10 m
		HT: 4.40 m
Ponte Osteria	42.874; 12.056	OT: 2.50 m
		MT: 3.80 m
		HT: 4.30 m
Mercatello	42.974; 12.266	n.d.
Palazzetta	42.970; 12.291	n.d.
Cannara	42.996; 12.584	OT: 2.20 m
		MT: 2.70 m
		HT: 3.00 m
Cantalupo	42.956; 12.597	OT: n.d.
		MT: 3.70 m
		HT: 3.90 m
Bevagna	42.944; 12.639	OT: 1.50 m
		MT: 2.40 m
		HT: 2.60 m
Foligno	42.950; 12.692	n.d.
Pale	42.984; 12.789	n.d.
Migianella	43.303; 12.249	n.d.
Montone	43.318; 12,314	n.d.
Trestina	43.359; 12.233	n.d.
Collepepe	42.930; 12.406	n.d.
Todi-Naia	42.766; 12.380	n.d.

SUPPLEMENTARY MATERIAL
Evaluating the response of hydrological stress indices using the CHyM model over a wide area in central Italy

Gorgabuia	43.586; 12.047	n.d.
Ponte Nuovo di Torgiano	43.009; 12.425	OT: 4.50 m
		MT: 6.00 m
		HT: 7.00 m
Ponte Felcino	43.127; 12.435	OT: 3.20 m
		MT: 4.00 m
		HT: 4.40 m
Pierantonio	43.260; 12.382	OT: 4.60 m
		MT: 5.10 m
		HT: 6.60 m
S. Lucia	43.422; 12.239	OT: 3.30 m
		MT: 3.70 m
		HT: 4.90 m
MIDDLE COURSE		
Visso	42.932; 13.081	OT: n.d.
		MT: n.d.
		HT: 2.20 m
Serravalle	42.779; 13.018	OT: 0.90 m
		MT: 1.00 m
		HT: 1.20 m
Ponte Buggianino	42.840; 12.948	n.d.
Alviano	42.584; 12.250	n.d.
Azzano	42.827; 12.760	OT: 0.90 m
		MT: 1.00 m
		HT: 1.20 m

La Bruna	42.820; 12.688	n.d.
Stimigliano	42.281; 12.559	n.d.
Tevere a Orte Scalo	42.441; 12.407	OT: 4.00 m
		MT: 6.00 m
		HT: 7.00 m
Vallo Di Nera	42.752; 12.851	OT: 1.10 m
		MT: 1.60 m
		HT: 2.00 m
Torre Orsina	42.572; 12.740	OT: 3.10 m
		MT: 3.80 m
		HT: 4.10 m
Velino a Terria	42.441; 12.796	OT: 6.00 m
		MT: 7.00 m
		HT: 8.00 m
Velino a Antrodoco	42.424; 13.068	OT: 0.80 m
		MT: 0.90 m
		HT: 1.05 m
Salto a S. Martino	42.322; 13.000	OT: n.d.
		MT: 1.80 m
		HT: n.d.
Ponte del Grillo	42.087; 12.602	OT: 5.00 m
		MT: 6.00 m
		HT: 7.00 m
Tevere a Nazzano	42.152; 12.644	n.d.
Tevere a Castelgiubileo	42.000; 12.491	n.d.

Tevere a Passo Corese	42.152; 12.661	n.d.
Tevere a Villa Spada	41.966; 12.508	n.d.
Tevere a Ponte Felice	42.356; 12.458	OT: 3.50 m MT: 5.00 m HT: 10.00 m
LOWER COURSE		
Tevere a Ripetta	41.915; 12.474	OT: 7.00 m MT: 11.00 m HT: 13 .00 m
Aniene a Ponte Salario	41.949; 12.508	OT: 2.50 m MT: 5.00 m HT: 7.00 m
Aniene a Subiaco	41.932; 13.085	OT: 2.70 m MT: 3.00 m HT: 3.50 m
Aniene a Marano Equo	42.000; 13.017	n.d.
Aniene a Ponte Lucano	41.966; 12.762	OT: 1.70 m MT: 2.20 m HT: 3.00 m
Aniene a Lunghezza	41.934; 12.678	OT: 3.00 m MT: 4.50 m HT: 6.00 m
Fosso di Pratolungo	41.949; 12.593	n.d.
Tevere a Ripetta	41.915; 12.474	OT: 7.00 m MT: 11.00 m

SUPPLEMENTARY MATERIAL
Evaluating the response of hydrological stress indices using the CHyM model over a wide area in central Italy

		HT: 13 .00 m
Rio Galeria	41.830; 12.339	n.d.
Tevere a Fiumara	41.746; 12.254	n.d.
Tevere a Porta Portese	41.881; 12.474	n.d.
Castiglione in Teverina	42.652; 12.234	n.d.
Tevere a Mezzocamino	41.813; 12.424	OT: 3.50 m
		MT: 5.00 m
		HT: 7.00 m
NORTHERN LAZIO COASTAL BASINS		
STATION NAME	**COORDINATES**	**CRITICALITY THRESHOLD**
Marta a Piantata	42.407; 11.881	n.d.
Marta a Tarquinia	42.254; 11.746	OT: 6.00 m
		MT: 7.00 m
		HT: 8.00 m
Rota	42.153; 12.000	n.d.
Arrone a Maccarese	41.881; 12.237	n.d.
LIRI-GARIGLIANO BASIN		
STATION NAME	**COORDINATES**	**CRITICALITY THRESHOLD**
Civitella Roveto	41.915; 13.426	n.d.
Sora	41.729; 13.627	OT: 3.00 m
		MT: n.d.
		HT: n.d.
Liri a Isola del Liri	41.678; 13.559	OT: 4.50 m
		MT: n.d.
		HT: n.d.

SUPPLEMENTARY MATERIAL
Evaluating the response of hydrological stress indices using the CHyM model over a wide area in central Italy

Liri a Ceprano	41.559; 13.525	OT: 2.50 m
		MT: 3.00 m
		HT: n.d.
Ceccano	41.610; 13.288	OT: 1.00 m
		MT: n.d.
		HT: n.d.
Sacco a Colleferro	41.763; 12.983	OT: n.d.
		MT: 4.00 m
		HT: n.d.
Anagni	41.712; 13.085	n.d.
Cosa ad Alatri	41.729; 13.356	n.d.

Table S1: list of hydrometers with available water stage recordings during the weather event, their location expressed in decimal degree coordinates and associated hydrometric criticality Thresholds for Ordinary criticality (OT), Moderate criticality (MT) and High criticality (HT). Where thresholds are not defined, the expression “n.d.” is reported.

S2 The Cetemps Hydrological Model (CHyM)

CHyM model is a distributed physical-based hydrological model, where all the relevant physical quantities are defined on an equally-spaced grid. The model can be used to simulate the hydrological cycle in any geographical domain with any spatial resolution, up to the resolution of implemented Digital Elevation Model (DEM), namely, 90 m in the current version. For operational purpose, the capability to simulate an arbitrary domain corresponds to the need to run the model for those river basins that are more stressed by the current meteorological event. CHyM recreates the surface drainage network from an arbitrary DEM matrix. The extraction of a coherent flow scheme is a fundamental step to simulate the hydrological cycle for a given geographical domain. In many distributed and lumped hydrological models (see as an example [53]) stream network is usually extracted using commercial or free Geographic Information System (GIS) software. According to the principle of minimum energy, CHyM assumes that the surface runoff occurs with a strong preferential direction following steepest DEM downhill gradient. Unfortunately, the application of this algorithm is affected by the occurrence of singularities due to the finite DEM resolution. CHyM model implements a cellular automata-based algorithm [52], in order to correct the sinks produced by the DEM singularities and obtain a coherent flow direction. The same approach is also used as a technique for spatializing and downscaling precipitation from point-data. A more detailed description of the cellular automata algorithm into the CHyM model can be found in [37].

S2.1 Surface Runoff

As for many other hydrological models (for a general reference see [54]) surface routing is calculated according to the kinematic wave approximation of the shallow water [55]. The equations used by CHyM model to simulate the surface routing overland and the channel flow are the continuity and momentum conservation equations:

$$\frac{\partial A}{\partial t} + \frac{\partial Q}{\partial x} = q$$

$$Q = \alpha A^m$$

where A is the flow cross-sectional area, Q is the flow rate of water discharge, q is the rate of lateral inflow per unit of length due to all the physical processes contributing the hydrological cycle, t is the time, x is the coordinate along the river path, α is the kinematic wave parameter and m the kinematic wave exponent, usually assumed = 1. The kinematic wave parameter α has the dimension of a speed and can be written as:

$$\alpha = \frac{\sqrt{S}\sqrt[3]{R^2}}{n(\mu)}$$

where S is the longitudinal bed slope of the flow element, n is the Manning's roughness coefficient depending on the land use type μ, R is the hydraulic radius that can be calculated as a linear function of the drained area D, according to:

$$R = \beta + \gamma D^{\delta}$$

β, γ and δ are empirical constants to tune during the calibration. The quantity D represents the area in the upstream of the flow element; in other words, with the previous equation, we assume that the cross section of a flow channel, in a generic point, can be calculated as a linear function of the upstream area (the exponent δ is usually ~1).

S2.2 Evapotranspiration

The potential evapotranspiration is computed as a function of the reference evapotranspiration, which is the evapotranspiration in soil saturation condition [56]), according to the formula:

$$ET_p = k_C ET_0$$

where k_c is the crop factor, which is a function of crop type. The reference evapotranspiration ET_0 is approximated as a linear function of temperature and is calculated according to:

$$ET_0 = \alpha + \beta N W_{ta}(h,T)T$$

where N is daily maximum sunshine hours, $Wta(h,T)$ is the compensation factor depending on the elevation h and the temperature T. The coefficients α and β need to be estimated and this is carried out through fitting the Thornthwaite formula with the least squared method:

$$16\frac{n(m)}{30}\frac{N(m)}{12}\left[10\frac{T(m)}{K_1}\right]^{K_2} = \alpha + \beta N W_{ta}(h,T)T$$

where $n(m)$ is the number of days of month m, N is the daily maximum sunshine hours for the month m, $T(m)$ is the monthly mean temperature, K_1 and K_2 are the thermal indices. The compensation factor $W_{ta}(h,T)$ is a function of the elevation and temperature, and is calculated from:

$$W_{ta}(h,T) = A(h)T^2 + B(h)T + C(h)$$

The coefficients $A(h)$, $B(h)$ and $C(h)$ have been estimated for different ranges of elevation according to the table reported by [57]. The actual evapotranspiration ET_A is indeed a fraction of the potential evapotranspiration ET_p and is calculated as a linear function of the ground relative humidity G_{RH}. More specifically, ET_A is zero in arid condition (G_{RH}<0.2) and is equal to ET_p for G_{RH}>0.7. For other values of ground humidity, the evapotranspiration term is calculated as a linear function of G_{RH}:

$$ET_A = \frac{GR_{RH} - 0.2}{0.7 - 0.2} ET_P = \frac{GR_{RH} - 0.2}{0.7 - 0.2} K_C ET_0$$

For other details about the estimation of the evapotranspiration term refer to [58,59].

SUPPLEMENTARY MATERIAL
Evaluating the response of hydrological stress indices using the CHyM model over a wide area in central Italy

S2.3 Melting

CHyM model implements a temperature-index melt model based on the assumption that the melting rates is given by the sum of two terms. The first term is linearly related to air temperature, which is regarded as an integrated index of the total energy available for melt. The second term is proportional to the incoming net solar radiation. Within this approach, the melting is assumed to occur when the temperature T is above a threshold level TT (typically 1°C). Pellicciotti et al. [60] recognized that this approach reproduces in a realistic way the observed melting rate in the Alpine region. The melting rate M (mm of equivalent precipitation per hour) is calculated following:

$$M = T_F T + S_{RF}(1-\alpha)G_{\downarrow}$$

The factor of proportionality for the first term T_F is the so called *temperature factor* (typical value ~0.05 mm/°C), the coefficient S_{RF} is the shortwave radiation factor and its typical value is ~0.0094 $mm/h\ M^2/(W°C)$, α is the fraction of solar radiation reflected by the surface, T is the ground temperature estimated by the CHyM model. In the previous formula $G_{\downarrow}$ is the incoming short wave solar radiation estimated as follows:

$$G_{\downarrow} = C_S A_{tr} sin\theta$$

In the latter equation, C_S is the solar constant (1,368 W/m^2) and A_{tr} the net sky trasmissivity that can be approximated by [61]:

$$\sin\theta = sin\varphi \cdot sin\delta_S - cos\varphi \cdot cos\delta_S \cdot \cos(\frac{2\pi t_{UTC}}{t_d} - \lambda)$$

Where t_{UTC} is the time of the day in Universal Time Coordinate and t_d is the length of the day. For practical purpose, the second term of melting contribute is considered only if the angle θ falls in the interval $0 \leq \theta \geq \pi/2$, i.e. during daytime. The solar declination angle, defined as the angle between the ecliptic and the plane of Earth's equator, for the Julian day d, it is given by:

$$\delta_s = \Phi_r \cos\left[\frac{2\pi(d - d_r)}{d_y}\right]$$

Where Φ_r is the tilt of Earth's axis relative to the ecliptic (Φ_r =23.45° = 0.409 radians), d_y is the year length (365 or 366 for leap years), d_r=173 is the Julian day corresponding to the Summer solstice. The values of temperature factor T_F and the shortwave radiation factor S_{RF} are calibrated through a "trial and error" process.

S2.4 Infiltration and percolation

The infiltration process is modelled using a conceptual model similar to those proposed by several authors [62,63]. Within this approach, the soil is schematized as two reservoirs of water: the precipitation infiltrates in the upper soil layer until the saturation level is reached. The water of the first reservoir (upper layer) also infiltrate (percolation) toward the lower soil layer. The total amount of water that infiltrates *I* is also saved at each time step in order to evaluate the return flow (see below).

S2.5 Return flow

Return flow is parameterized assuming that the contribute to each elementary channel-cell is proportional to the total infiltration in the upstream basin in the last *N* months

$$R_f = \int_{UP} ds \int I(t,s)dt$$

the infiltration term *I,* described in the previous paragraph, is integrated over the whole upstream basin (UP) of each cell and the time integral is carried out over the last *N* months, being *N* a value to be optimized during the calibration process. We assume that the infiltrated water contributes to the return flow within the same catchment. The return flow is then calculated, for each cell, as a linear function of the R_f term, and the linear coefficient is optimized during the calibration phase with typical values ~$5 \cdot 10^{-7}$ mm $hour^{-1}$ km^{-2}.

SUPPLEMENTARY MATERIAL

Evaluating the response of hydrological stress indices using the CHyM model over a wide area in central Italy

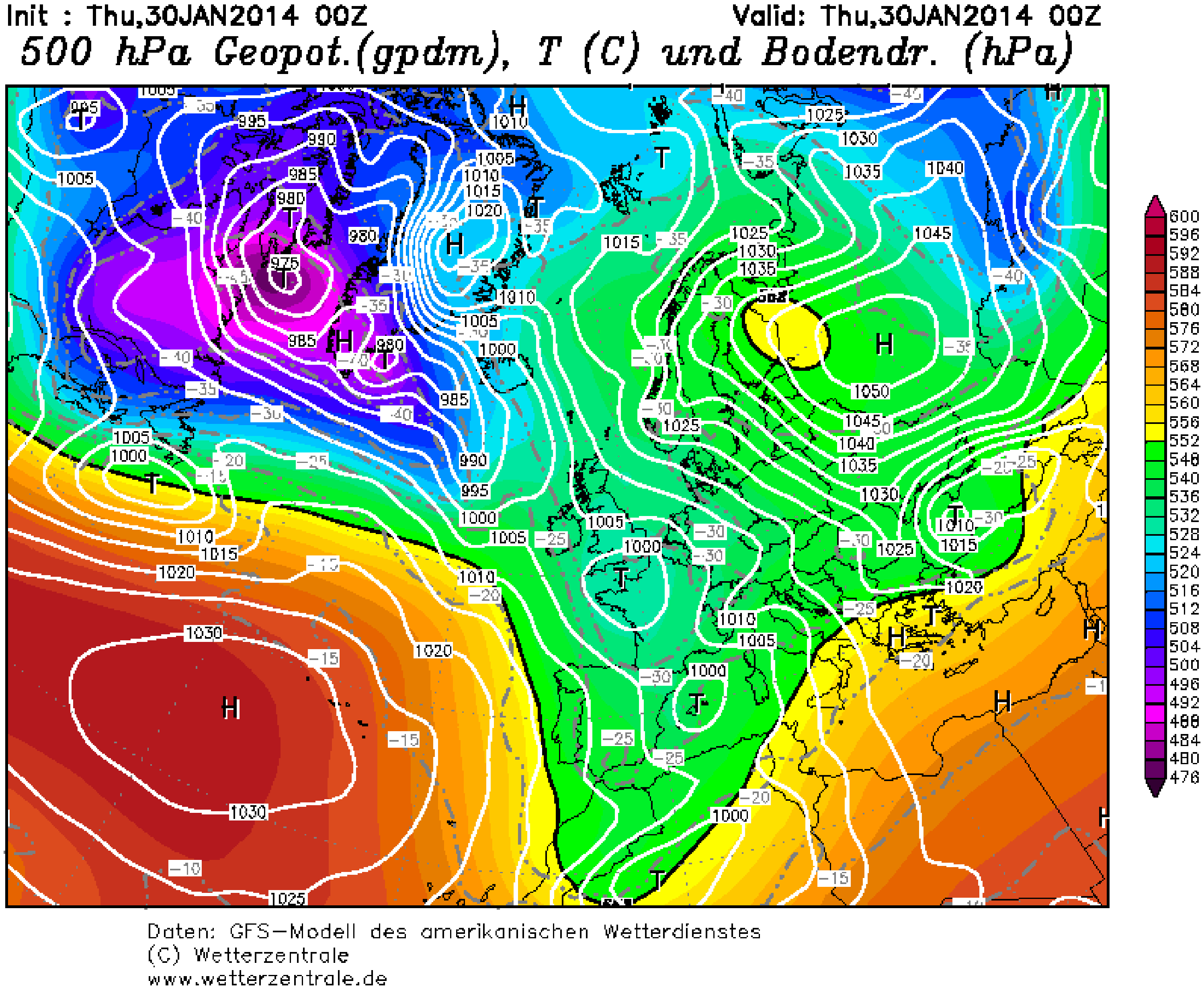

SUPPLEMENTARY MATERIAL

Evaluating the response of hydrological stress indices using the CHyM model over a wide area in central Italy

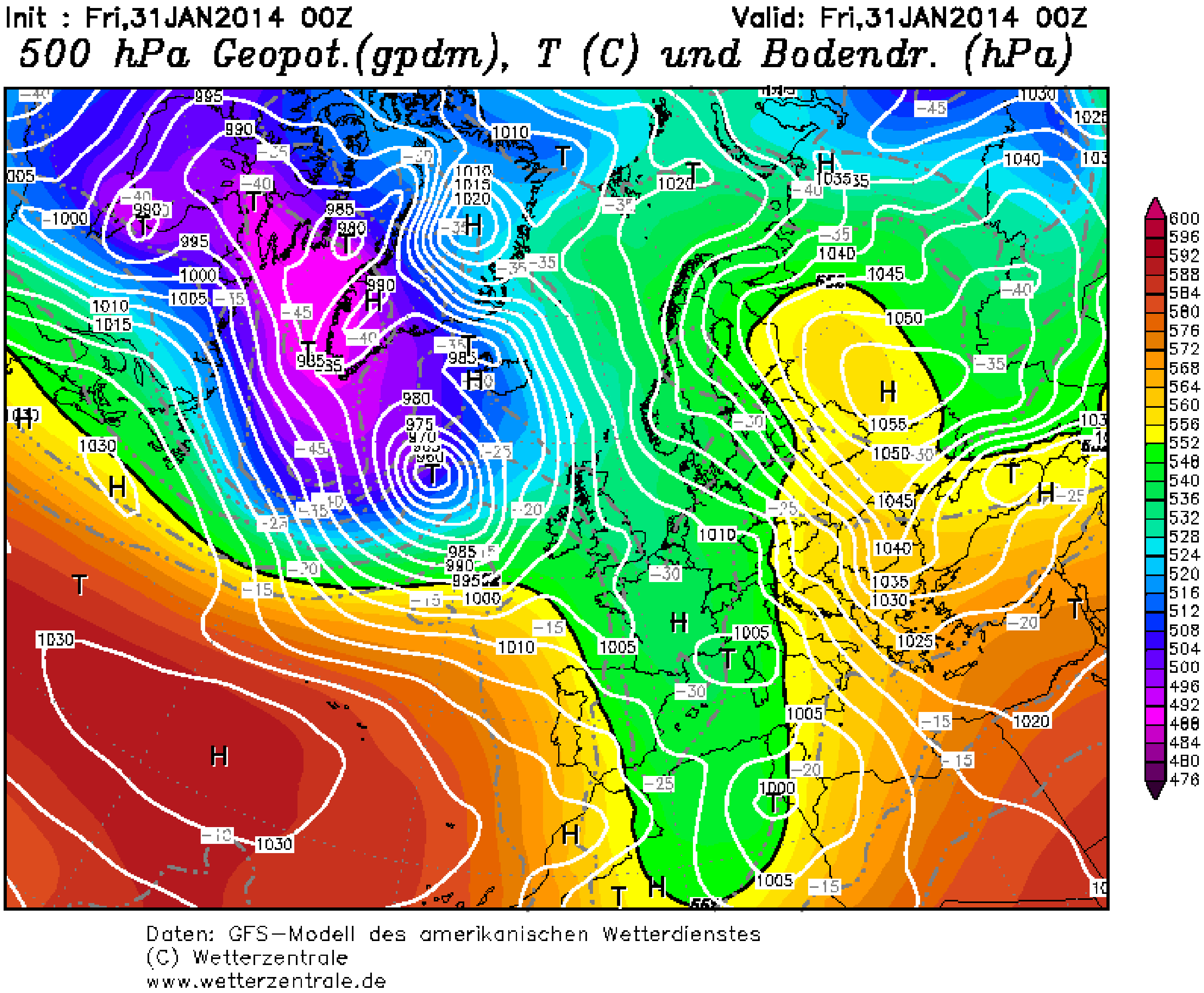

SUPPLEMENTARY MATERIAL

Evaluating the response of hydrological stress indices using the CHyM model over a wide area in central Italy

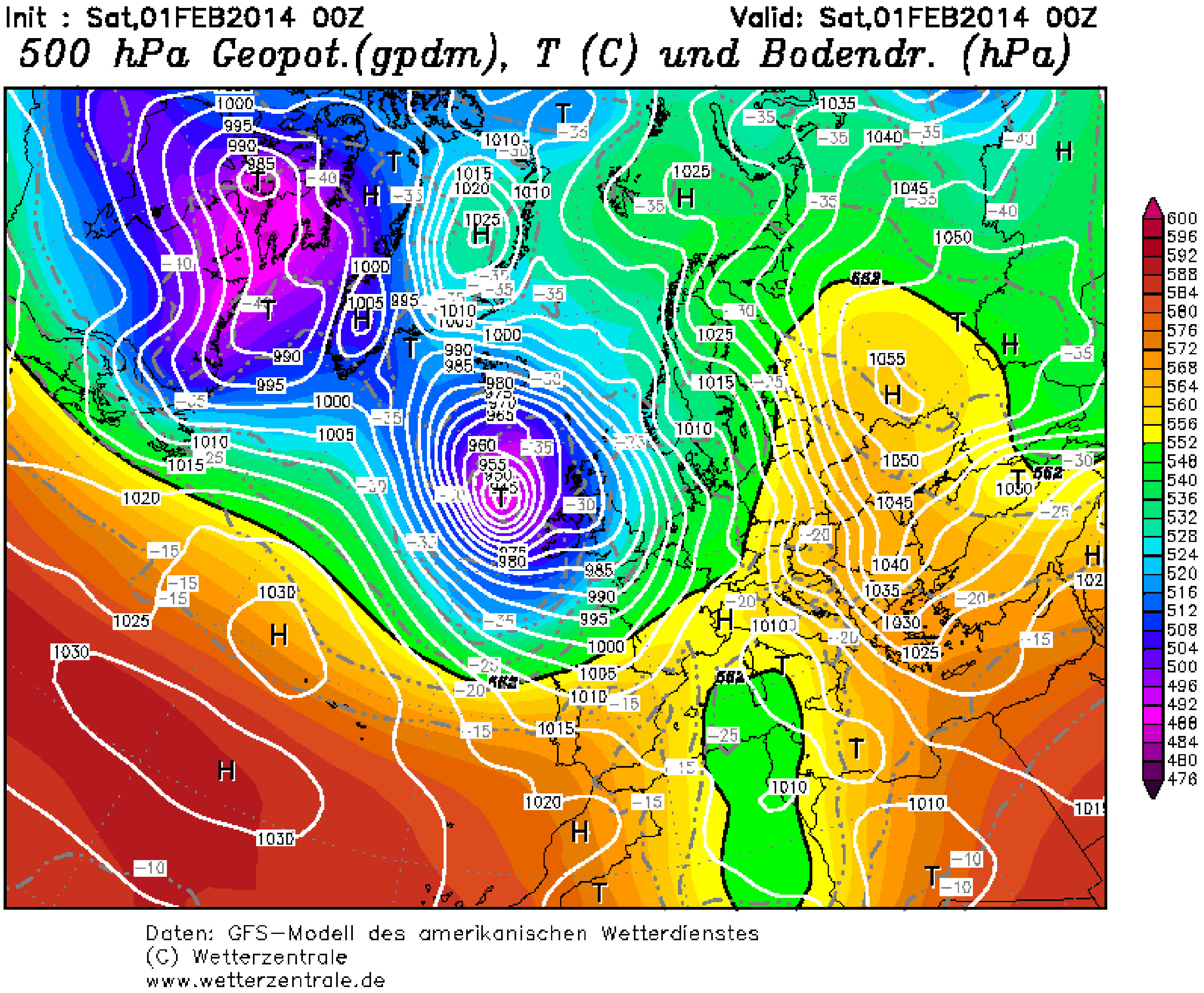

SUPPLEMENTARY MATERIAL

Evaluating the response of hydrological stress indices using the CHyM model over a wide area in central Italy

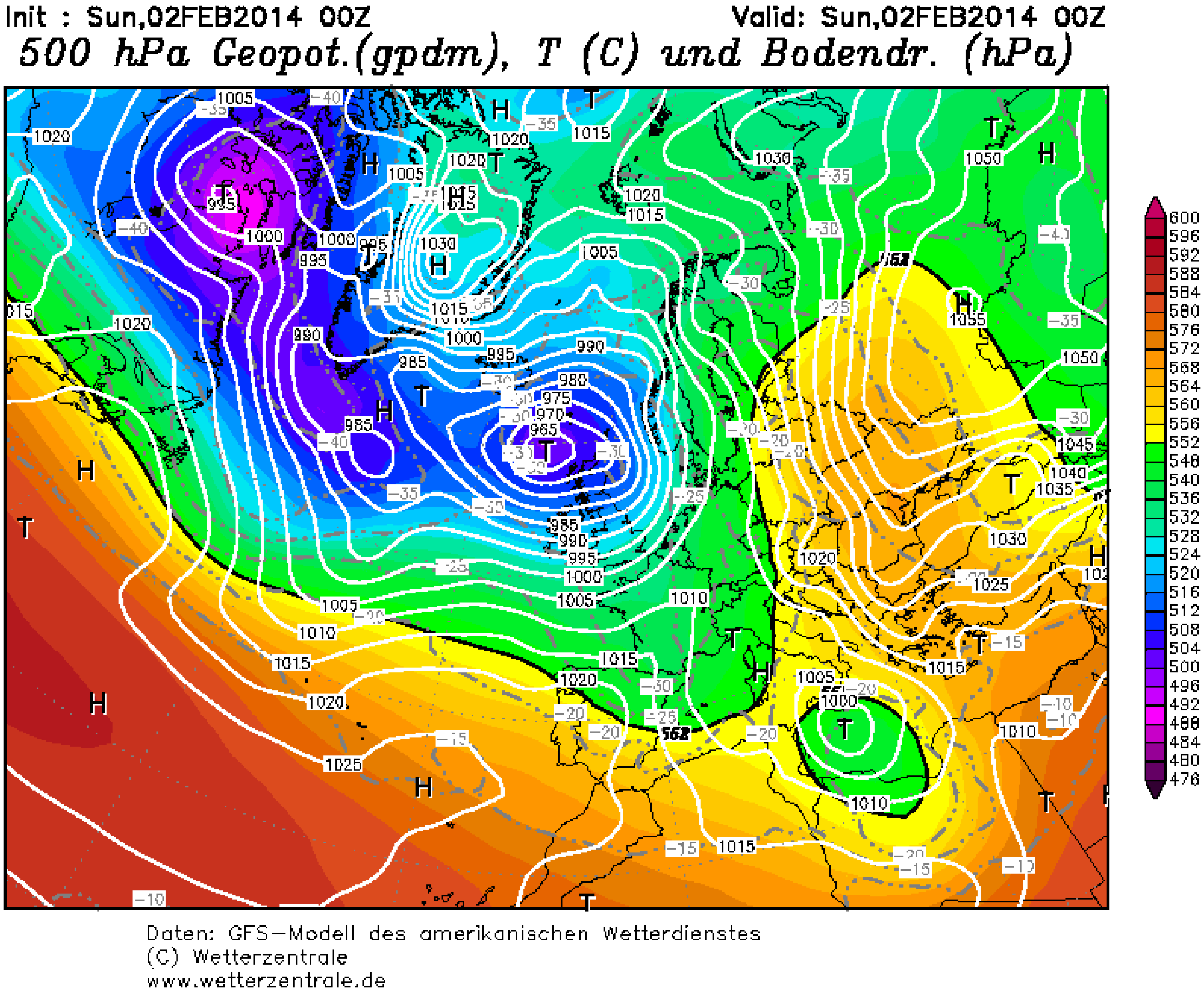

SUPPLEMENTARY MATERIAL

Evaluating the response of hydrological stress indices using the CHyM model over a wide area in central Italy

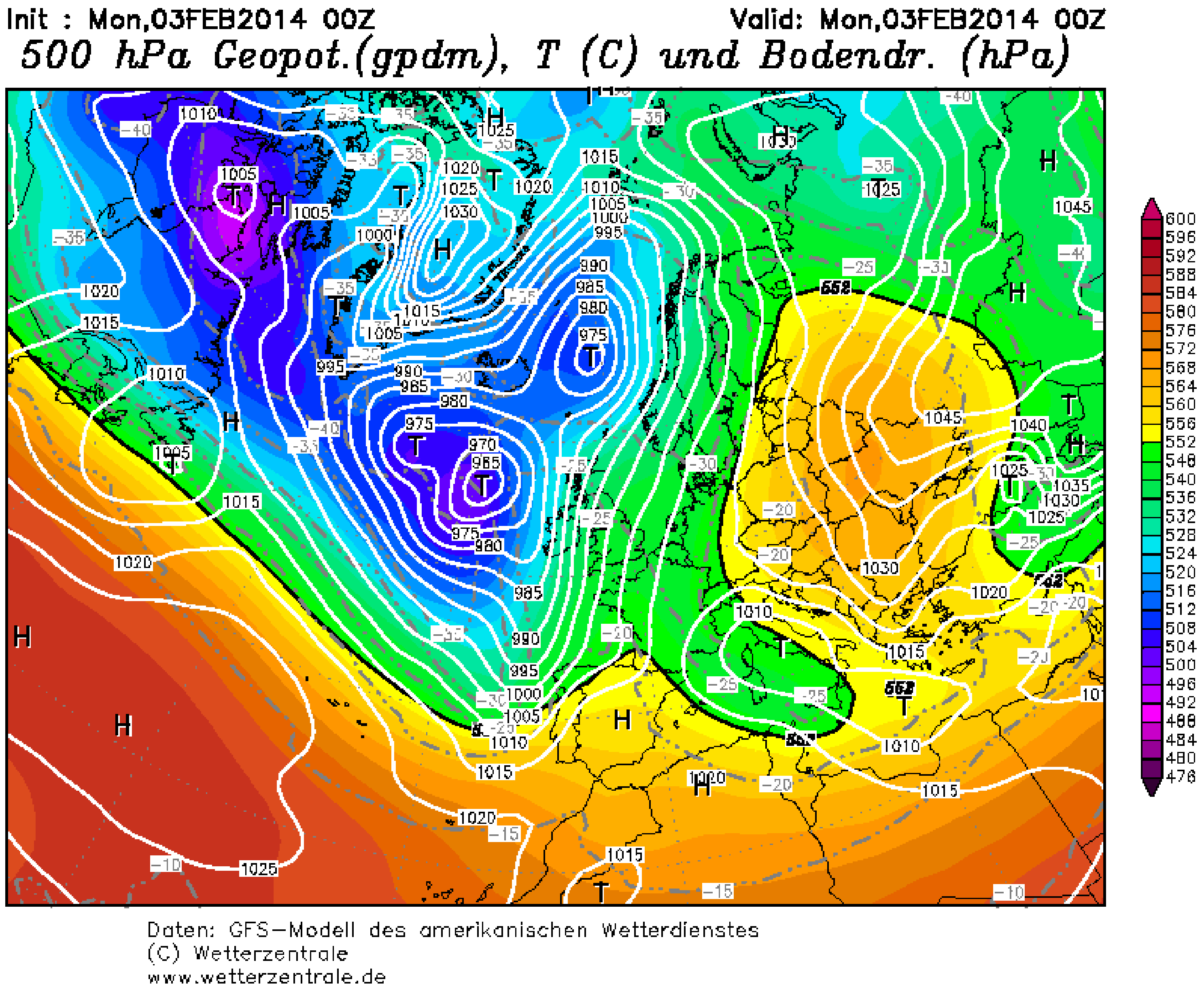

SUPPLEMENTARY MATERIAL

Evaluating the response of hydrological stress indices using the CHyM model over a wide area in central Italy